Hindawi
Journal of Food Biochemistry
Volume 2023, Article ID 8890518, 17 pages
https://doi.org/10.1155/2023/8890518

Research Article

Total Flavone Content of *Cydonia oblonga* Miller Inhibits Proliferation and Migration of Renal Carcinoma Cells by Inhibiting the S1PR2/FAK Pathway

Muhadaisi Nuer,[1] Nawaz Khan,[1] Bentuo Zhang,[2] Kayisairer Abdurousuli,[1] Houqing Yin,[2] Dan Wang,[2] Jimilihan Simayi,[1] Nulibiya Maihemuti,[1] Ziruo Talihati,[1] Sendaer Hailati,[1] Zequn Wang,[2] Mengyuan Han,[1] Ainiwaer Wumaier,[1] Yan Ribai,[3] Wenting Zhou ,[1] and Yan Pan [2]

[1]*Department of Pharmacology, School of Pharmacy, Xinjiang Medical University, No. 393, Xinyi Road, Urumqi 830011, Xinjiang, China*
[2]*Department of Pharmacology, School of Basic Medical Sciences, Health Science Center, Peking University, Beijing 100191, China*
[3]*School of Pharmaceutical Sciences, Peking University, Beijing 100191, China*

Correspondence should be addressed to Wenting Zhou; zwt@xjmu.edu.cn and Yan Pan; pannay26@bjmu.edu.cn

Received 6 December 2022; Revised 24 January 2023; Accepted 10 February 2023; Published 30 March 2023

Academic Editor: Jae Young Je

Copyright © 2023 Muhadaisi Nuer et al. This is an open access article distributed under the Creative Commons Attribution License, which permits unrestricted use, distribution, and reproduction in any medium, provided the original work is properly cited.

Cydonia oblonga Miller (*C. oblonga*) is known for its beneficial properties for health since ancient times. *C. oblonga* has also been shown to possess antihemolytic, antidiabetic, and antilipoperoxidation, as well as lipid-lowering properties. Modern research has shown that *C. oblonga* also possess antitumor effects. However, studies have not reported whether its main compounds inhibit renal cell carcinoma (RCC) development and progression. We found the inhibitory effect of total flavone of *C. oblonga* (TFCOM) in RCC cells through *in vitro* screening tests. The molecular mechanism of this effect is still unknown. Therefore, molecular docking combined with network pharmacological methods was used in order to clarify the molecular mechanisms of TFCOM anticancer effects. TFCOM showed potent inhibitory effects on the proliferation and migration of 786-O and Renca cells. Hoechst 33342 staining test results indicated that TFCOM's cell growth inhibition in RCC cells may be mediated through apoptosis. It may significantly influence S1PR2/FAK, WNT/β-catenin, and PI3K/AKT/mTOR signaling pathways that can regulate a series of cellular activities and can participate in the processes of cell proliferation, migration, and apoptosis. We conclude that TFCOM has antitumor activity against kidney cancer. It may induce apoptosis and inhibitory effects on cell proliferation and migration through S1PR2/FAK, WNT/β-catenin, and PI3K/AKT/mTOR signal pathways. TFCOM might be a potential anticancer drug to be further developed for human kidney cancer therapy. In recent years, many synthetic drugs with anticancer effects have the disadvantages of high price and side effects. Thus, the development of anticancer drugs from natural resources has its application value. Our results suggest that TFCOM, as a natural product, has multiple target effects, and it may act through proteins and receptors such as FAK and S1PR2, thereby affecting the activation of downstream proteins and inhibiting the occurrence and development of renal cancer cells.

1. Introduction

Renal cell carcinoma (RCC) represents the cancer type that originates in the renal epithelium cells. More than 90% of kidney cancer cases are diagnosed as RCC with 400,000 cases and 175,000 deaths in 2018. RCC is enlisted among the 10 most common cancer types worldwide [1]. RCC consists of several diverse cell types with different histological, genetical, biological, and behavioral properties. The identification of the genes affecting to inherited syndromes with RCC has provided much of our knowledge of the molecular basis of early sporadic RCC. Most of the genes that result in the

dysregulation of cellular pathways after mutation like oncogenes and tumor suppressor genes are still remained to be identified and explained in RCC [2]. Tyrosine kinase inhibitors and VEGF antibodies are widely used as first-line and second-line therapies for renal cell carcinoma. In clinical experiences, it is noticed that RCC inhibited with multiple drugs acting on different targets results better as compared to the single medicinal agent approaches [3, 4]. However, these practices were found to off target high-toxicity rates as compared to their curing effect. For instance, sunitinib combined with everolimus therapy in metastatic RCC patients was noticed to have severe toxicity [5]. Currently, the facts claim that approximately 40% of RCC patients will die due to their disease severity because it is hard to manage with the available treatment products highlighting the necessity of additional research work.

The products derived from different natural sources contain the tendency to stimulate different physiological pathways which may help in curing life-threatening diseases like cancer [6]. In the last few years, effective therapy for cancer treatment became a challenging situation, and different strategies were set against cancer treatment. One of these strategies which gained the attraction of researchers was the exploration of plant-derived compounds. Different researchers investigated the effect of phytochemicals against cancer [7, 8]. These plants-derived extracts were found with the potential for treating cancers with low toxicity. Among these plants, *Cydonia oblonga* Miller (*C. oblonga*) also known as quince which belongs to Rosaceae family is a medicinal plant that contains high effective phenolic profile as well as other medicinal important compounds like polysaccharides and steroids [9]. The plant is used both as a medicinal and food agent [10]. Different parts of the plant have been reported to be used as folk medicines for different disease treatment. Leaves decoction was used as antipyretic and antidiarrheic and to cure sore throat [11], whereas jelly-like consistency resulted from boiled seeds. Mucilage was popular for its laxative and sedative effects and it was used topically to treat minor burns [12]. On the other hand, in traditional Uyghur medicines, the plant is used to cure hypertension and cardiovascular diseases [13]. While in Iranian traditional medicine, the plant has several traditional medicinal uses including liver protection, stomach tonic, nausea and vomiting, chronic headache, heart palpitation, and motion sickness [14]. Pharmacological studies have demonstrated that *C. oblonga* presents potential anticancer properties [15]; most of the bioactive compounds existing in *C. oblonga*, such as quercetin, rutin, and kaempferol, have been reported to exhibit anticancer effects. However, the anticancer mode and mechanism of action of total flavone of *C. oblonga* (TFCOM) are not fully understood. Moreover, different studies reported the plant as an effective source against treating hypertension [16], gastric diseases [17], hyperlipidemia [18], and diabetes [19].

In the current study, we examined the antitumor effects of TFCOM on kidney cancer cells and investigated its mechanisms. We observed that TFCOM may induce apoptosis and inhibitory effects on cell proliferation and migration through S1PR2/FAK, WNT/β-catenin, and PI3K/AKT/mTOR signal pathways.

2. Materials and Methods

2.1. TFCOM Extraction Method. The fruits were collected from Kashgar county, Xinjiang, China, and identified by Prof. Palida Abliz, Department of Pharmaceutical Chemistry and Pharmacognosy, Xinjiang Medical University, China. A voucher specimen (no. TCMEHSM2013_101) was deposited in the Department of Traditional Chinese Medicines Ethnical Herbs Specimen Museum of Xinjiang Medical University. The fruits were washed with tap water cut into thin slices and shade dried. After complete drying, the fruits were crashed into powder by electric blender and extracted by ultrasonic extraction (2 times) in 60% ethanol (1 : 10) for 40 minutes (each time). The filtrate was concentrated with a rotary evaporator until complete removal of ethanol. The extract was loaded onto a chromatographic column containing AB-8 macroporous adsorption resin washed twice with water to elute the polysaccharide components and collected with 50% and 95% ethanol. The purified extract was combined, concentrated, freeze-dried, and stored at −20°C until the next use. The content of flavonoids in the extract was determined using a UV spectrophotometer with rutin as the standard. Finally, the content of flavonoids in the extract of *C. oblonga* could reach more than 40%.

2.2. Cell Culture. Human 786-O renal cells and murine renal (Renca) cells were purchased from Procell Life Sciences and Technology Co., Ltd. (Wuhan, China). The MDCK cells were gifted for the experiment by Mr. Yang bao Xue from the School of Basic Medicine, Peking University. The H1975 and A549 cells were obtained from the cells bank of the Pharmacology Department of Peking University. Renca cells were cultured in a specifically prepared medium (Product no. CM-0568) provided by Procell Life Sciences and Technology containing RPMI-1640, NEAA, L-glutamine, sodium pyruvate (1 mM), FBS (10%), and penicillin streptomycin (1%). Human 786-O cells were cultured in RPMI-1640 medium supplemented with FBS (10%) and penicillin streptomycin (1%). The MDCK, H1975, and A549 cells were cultured in DMEM high glucose supplemented with 10% FBS and 1% penicillin streptomycin. All cells were kept at 37°C in a humidified incubator with 5% CO_2 supply.

2.3. Cell Proliferation Assay. The cell viability assay was evaluated by using the cell counting kit-8 (CCK-8, Bioss, China) assay. 5.0×103 cells per well were seeded in 96-well plates, after 24 hours the cells were treated with different concentrations of TFCOM (20, 40, 80, 160, 320, and 640 μg/mL) and incubated for 48-hour period at 37°C in a humidified incubator with 5% CO_2 supply. Readings were taken in triplicate at 450 nm wavelength with a microplate reader (Multiskan GO, Thermo Fisher Scientific).

2.4. Cell Migration

2.4.1. Transwell Assay. The experiment was performed in a 24-well plate containing chambers of Transwell membrane filter (8 μm, Corning Inc., 3470). Both Renca and 786-O cells were suspended in serum-free medium at 3×10^4 cell/mL concentration. The cells were seeded on the upper chamber of the container for 12 hours. Subsequently, the cells were stained with crystal violet staining solution (Beyotime Biotech) and were visualized and photographed by an inverted microscope for migration assay.

2.4.2. Wound Healing Assay. 786-O and Renca cells were immediately seeded into a 6-well plate with a density of 6×10^5 cells per well. After complete confluence of cells, a perpendicular "I" shape scratch was drawn in each well of the 6-well plate with the help of a sterile pipette tip of 200 μl. Next, the cells were treated with different concentrations (0, 40, 80, and 160 μg/ml) of TFCOM. After 12- and 24-hour incubation period, the width of the scratch was observed and photographed under an inverted microscope. The cell migration rate was calculated by using the following formula:

$$\text{Cell migration rate}\,(\%) = \frac{(0\,\text{h scratch spacing} - 12 \text{ or } 24\,\text{h scratch spacing})}{0\,\text{h scratch spacing}} \times 100\%. \quad (1)$$

2.5. Cell Apoptosis Assay. Hoechst 33342/PI (Solarbio, CA1120) double-staining method was performed to observe the apoptotic rate of 786-O and Renca cells by following a standard method [20]. Briefly, different concentrations (40, 80, and 160 μg/mL) of TFCOM were added to the cells and incubated for 48 hours, after rinsing the cells with PBS. 5 μL of Hoechst 33342 and PI were added and incubated for 20 min at 37°C. After stimulation, the cells were rinsed 3 times with PBS and observed under a Leica DMi8 inverted fluorescence microscope (Leica Microsystems, German) for morphological alterations. The cells stained with Hoechst 33342 appeared with blue fluorescence, whereas cells stained with PI manifested red fluorescence. Normally, Hoechst 33342 can normally be penetrated through the cell membrane while the PI can just only cross a damaged cell membrane. The apoptotic rate and necrotic rate of 786-O and Renca cells were identified as the percentages of apoptotic cell nuclei and necrotic cell nuclei in five random fields.

2.6. Network Construction and Analysis

2.6.1. Screening of TFCOM-Active Components. In our previous studies, 11 active components were collected from *C. oblonga* based on the literature published by our research group, including isoquercetin, quercetin 3-galactoside, ursolic acid, sitosterol, rutin, amygdalin, β-carotene, chlorogenic acid, quercetin, kaempferol, catechin, and other compounds [21].

2.6.2. Prediction and Screening of Active Targets Corresponding to Active Components. Identifying potential active molecules is a key step in drug research. When using experimental methods to find drug targets, it is difficult to find the target comprehensively due to the complex environment of the organism and prolonged time consumption. Through the TCMSP analysis platform and the Swiss TargetPrediction database, the relevant targets corresponding to the active ingredients (selection score > 0.5) were screened (https://www.swisstargetprediction.ch). The target was transformed from gene name to protein name by UniProt database, and the duplicate target name was deleted. Active ingredients and predicted targets were used to construct a compound-target (C-T) network by Cytoscape8.0 software.

2.6.3. Ingredient-Target Network Construction. A Venn diagram of the interconnected gene symbols was obtained after intersecting the drug-related targets with disease-related targets. Next, based on the interaction of bioactive components of TFCOM, gene symbol, and the disease (renal cell carcinoma), a complex informational network was built. For visual analysis of the drug-component-target-disease network, Cytoscape 3.8.2 software was used.

2.6.4. Gene Ontology (GO) and Kyoto Encyclopedia of Genes and Genomes (KEGG) Pathway Enrichment. The enrichment of GO analysis and KEGG pathway was employed by using Bioconductor (R) v3.8 bioinformatics software (https://bioconductor.org/). Terms with expression analysis systematic explorer scores of ≤0.05 were collected for functional annotation clustering. The pathway enrichment analysis was performed using the KEGG database to verify the functional categories of statistically significant genes ($p < 0.05$). Terms with thresholds of a count of ≥ 2 and expression analysis systemic explorer scores of ≤ 0.05 were screened for functional annotation clustering.

2.7. Western Blot Assay. To perform the experiment, cells were cultured in 6-well plates after full confluence; TFCOM was added at different concentrations (40, 80, and 160 μg/mL) for 48 h. After 2 days of incubation, the total protein was extracted from 786-O and Renca cells by using RIPA Lysis Buffer (Thermo Fisher, Shanghai, China). Next, the total protein concentration was determined with the BCA protein assay kit (Biorigin, BN27109-500T). For protein expression analysis, 20 μg of protein was loaded to SDS-PAGE. The obtained protein sample was then transferred to a PVDF membrane and blocked for 1 hour with skimmed milk (5%) at 37°C. After that, the membrane was washed three times with TBST and incubated overnight with primary antibodies

at 4°C. Next, the membrane was washed again with TBST for three times and incubated with secondary antibodies (40295, anti-rabbit IgG; 40296, anti-mouse IgG, cell signaling technology) at room temperature for two hours. For visualization of proteins, an enhanced chemiluminescent SuperSignal West Pico Kit (34577, Thermo Fisher Scientific) was used. The exposure and development of image were performed by using ChemiDoc imaging system. GAPDH (BN20621, Biorigin) was used as an internal control. Image J software was used to measure and analyze the protein bands.

2.8. Statistical Analysis. The results are represented as mean ± SD. Statistical significance between the different groups was analyzed by one-way ANOVA using GraphPad Prism 8.4 (GraphPad 8.4 Software, Inc., San Diego, CA, USA). The comparisons between the control and treated groups were performed by one-way analysis of variation (ANOVA) followed by Dunnett's multiple comparison test. Significance was accepted at p value lower than 0.05.

3. Results

3.1. TFCOM Inhibited Proliferation in Cancer Cell Lines. To determine the antiproliferative effect of TFCOM, several types of cancer cell lines such as 786-O, Renca, H1975, A549, MCF-7, and MDCK were incubated with different concentrations of TFCOM (10, 20, 40, 80, and 160 μg/mL) for 48 hours. The result obtained by the CCK-8 assay confirms the cell growth inhibitory effect of TFCOM extract (Figures 1(a)–1(f)). The extracts from quince showed concentration-dependent growth inhibitory activity toward different cancer cells. Among them, 786-O and Renca cells were the most sensitive, followed by breast cancer cells MCF-7, while the TFCOM was found to be ineffective against nonsmall-cell lung cancer cells (A549). However, the TFCOM was observed with producing no toxicity to MDCK cells (Madin–Darby Canine Kidney). Therefore, we chose 786-O and Renca cells as the main research targets. In conclusion, the TFCOM could inhibit the proliferation of 786-O and Renca cells in a dose-dependent manner. With the increase in the concentration, the cell inhibition rate was continuously enhanced and the calculated IC50 value was 93.19 μg/mL and 62.54 μg/mL with 48 h incubation, respectively (Figures 1(g) and 1(h)).

3.2. TFCOM Inhibited Migration of 786-O and Renca Cells. Migration ability of tumor cells is an important indicator for the evaluation of the malignancy of cancers *in vitro*. To assess if TFCOM affects cell migration *in vitro*, wound-healing assay and Transwell assays were performed. The transwell assay showed that TFCOM significantly reduced the migration of 786-O and Renca cells in a dose-dependent manner (Figures 2(a) and 2(b)). The wound-healing assay showed that the migration distance of 786-O and Renca cells treated with TFCOM was significantly shorter as compared to the blank group (Figures 2(c) and 2(f)). After being treated with 80 and 160 μg/mL TFCOM for 24 h, the cell migration of 786-O and Renca cells was inhibited. TFCOM had a concentration-dependent inhibitory effect on cell migration. Among them, the 160 μg/mL group had the shortest migration distance, invasion capability was decreased to 27.8 ± 3.2% compared to that of the control ($p < 0.001$). Together, these results suggested that TFCOM influenced tumorigenesis of RCC by inhibiting migration and invasion of RCC cells.

3.3. TFCOM Promotes Apoptosis of 786-O and Renca Cells. Apoptosis, which is characterized by chromatin condensation and nuclear shrinkage, is identified by blue fluorescence following staining with Hoechst 33342/PI. In contrast, red fluorescence indicates necrotic cells due to the penetration of PI. In comparison to the control group, the TFCOM-stimulated group was found with more necrotic and apoptotic cells (Figure 3). At 160 ug/mL concentration, the TFCOM significantly promotes apoptosis of 786-O and Renca cells (Figures 3(a) and 3(d)). Besides, we also checked some protein expressions by western blotting that is associated with apoptosis. Results indicated that the ratio of PARP, caspase-3, and Bcl-2 was decreased while the expression of cleaved-caspase-3, cleaved-PARP, and the protein level of Bax was increased, which suggested that TFCOM induces cell apoptosis (Figures 3(c) and 3(f)). Collectively, these results suggested that TFCOM significantly induces apoptosis of 786-O and Renca cells.

3.4. Network Analysis

3.4.1. Prediction and Screening of Active Targets Corresponding to Active Components. Screening through the TCMSP analysis platform and the Swiss TargetPrediction database to obtain the relevant target corresponding to the active ingredient (selection score > 0.5), the target is converted from the gene name to the protein name through the UniProt database, and the duplicate target name is deleted, and 259 targets are obtained (Figure 4(a)).

3.4.2. Analyses of the Drug-Ingredient-Gene Symbol-Disease Network. A total of 207 gene symbols were related to the disease, and 195 gene symbols were found in relation to the drug (Figure 4(b)). Among them, 64 genes were overlapped which proposes that these overlapped genes may be involved in the anticancer activity of the TFCOM.

3.4.3. Protein-Protein Interaction Network of TFCOM Extract-Related Cancer Targets. Natural products exhibit a range of pharmacological activities due to their complex nature and instant synergetic effect on different targets. In the current study, we tried to investigate the potential anticancer mechanism of TFCOM. For this, a protein-protein interaction (PPI) network was constructed for the TFCOM bioactive compounds and targeted proteins. Figure 4(c) represents that the PPI network consists of 59 nodes and 215 edges. The light blue edges shown in the figure represent interactions reported from the database. Green indicates predicted interactions with neighborhood genes. Red

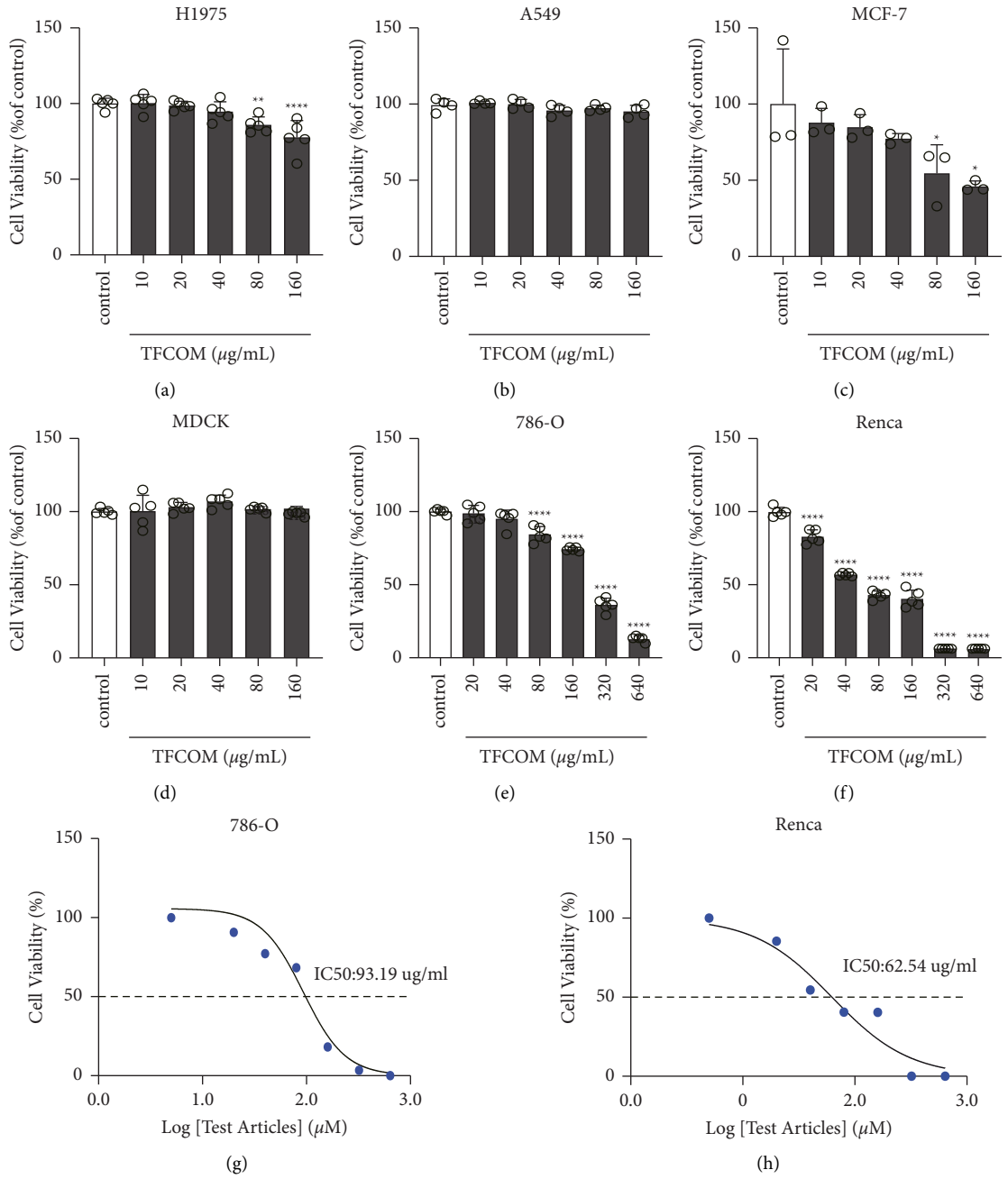
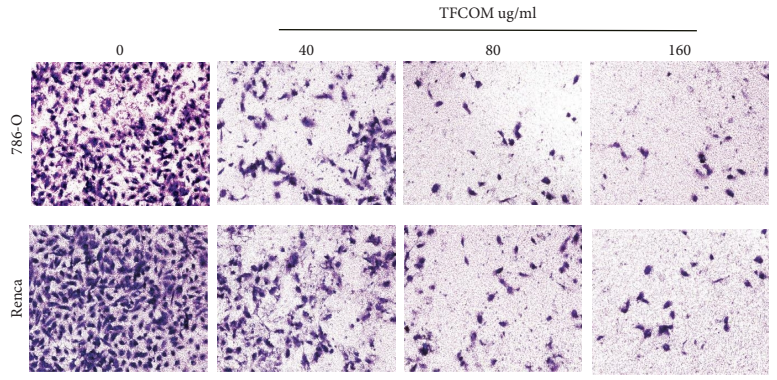
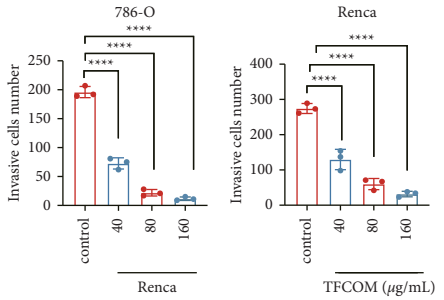


Figure 1: TFCOM inhibited the proliferation of 786-O and Renca cells. (a–c) H1975, A549, and MCF-7 cells were treated with 10, 20, 40, 80, and 160 μg/ml of TFCOM for 48 h; (d) MDCK cells were exposed to the indicated doses of TFCOM for 48 h. 786-O and Renca cells were treated with 20, 40, 80, 160, 320, and 640 μg/ml of TFCOM for 48 h (e, f); IC50 of TFCOM on 786-O and Renca cells in 48 h (g, h). Cell viability was analyzed by CCK-8 assay, and the surviving cells were determined and presented as a percentage of the nontreated cells. Data are presented as mean ± standard deviation (SD) in three independent experiments. $^{*}p < 0.05$, $^{***}p < 0.001$, $^{**}p < 0.01$ and $^{****}p < 0.0001$, as compared with the nontreated control.

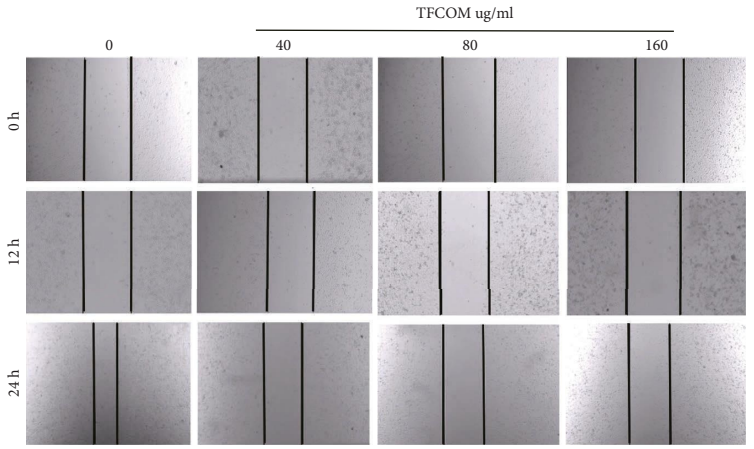
represents interactions based on gene fusion predictions. Dark blue shows the predicted interactions of gene co-occurrence. Yellow represents predicted interactions in text mining. Purple represents interactions based on protein homology predictions. The degree of nodes indicates the potency of the bioactive compound and the target in a network; therefore, nodes with higher degrees may be more important in pharmacological processes. In addition, we also found the 10 central genes, including p53, AKT, MYC, MAPK, Bcl-2, CTNNB1, CASP3, CASP8, BAX, and BCL2L1. In the biological process, these central genes are significantly enriched in tumor cell proliferation, migration, and apoptosis. Among them, p53 is known as a tumor suppressor protein and transcription factor. It mainly regulates cell division, prevents the cells from DNA mutation or damage from dividing, and transmits apoptotic signals to



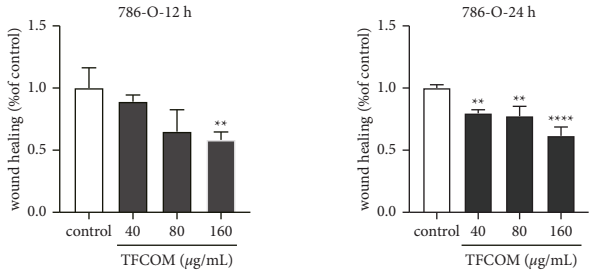
(a)



(b)



(c)



(d) (e)

Figure 2: Continued.

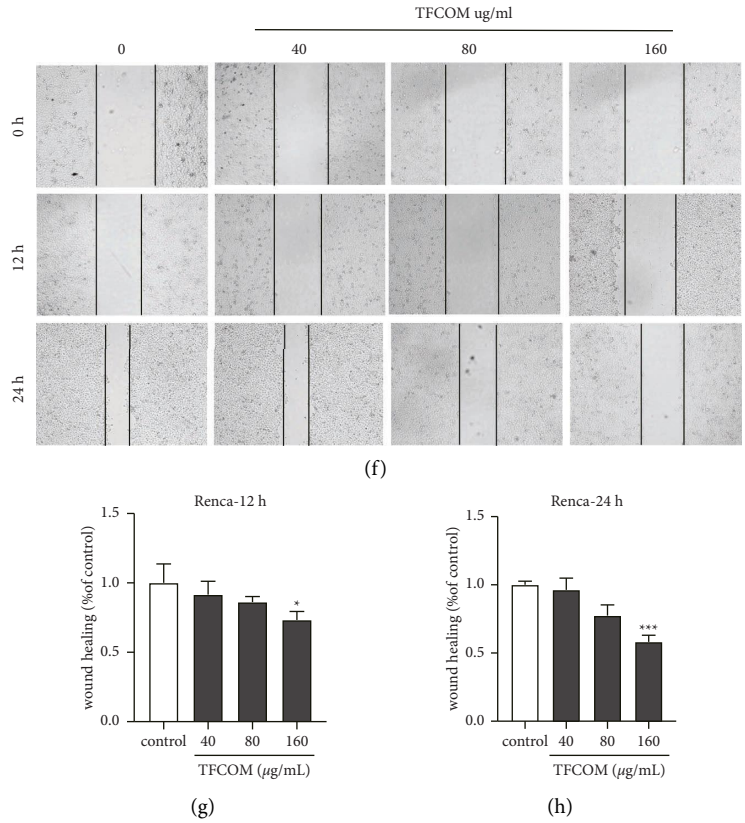


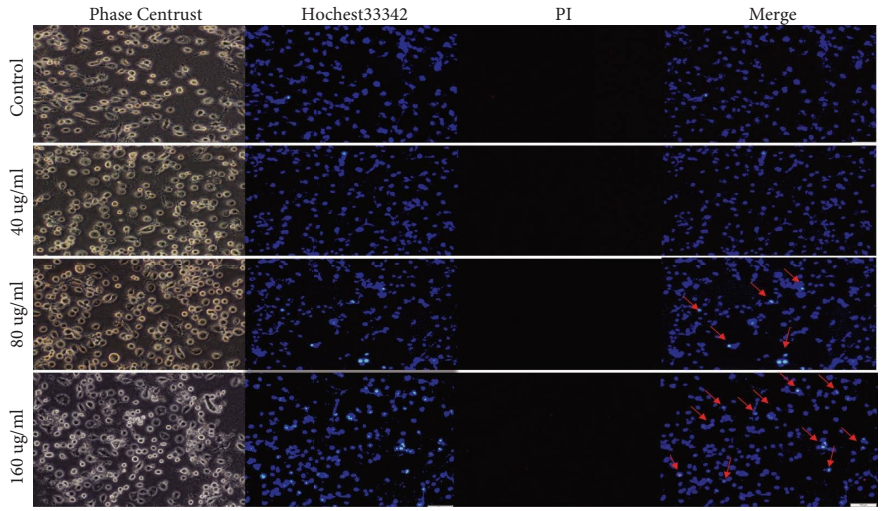
Figure 2: TFCOM inhibited the migration of 786-O and Renca cells. (a) Transwell assay showed that TFCOM inhibited migration of 786-O and Renca cells. Scale bar $= 100\,\mu$m. (b) A number of migratory cells. Data are presented as mean ± standard deviation (SD) in three independent experiments. $^{*}p < 0.05$, $^{***}p < 0.001$ as compared with the nontreated control. (c) 786-O cells were analyzed for cell migration using a wound healing assay (magnification, x100). (d, e) The determined migration ability of 786-O was subsequently quantified as the percentage of the control. (f) 786-O cells were analyzed for cell migration using a wound healing assay (magnification, x100). (g, h) The determined migration ability of 786-O was subsequently quantified as the percentage of the control. Results are presented as mean ± SD in three independent experiments. $^{*}p < 0.05$, $^{**}p < 0.01$, and $^{***}p < 0.001$ as compared with the nontreated control.

these cells through transcriptional regulation because of which tumor formation is prevented. We further detected the effects of TFCOM on 786-O and Renca cells by western blot, and the results showed that TFCOM could promote the expression levels of p53 in 786-O and Renca cells (Figure 4(d)).

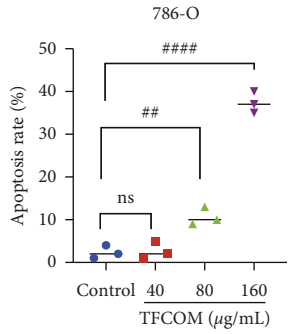
3.4.4. GO and KEGG Pathway Enrichment Analyses. For the verification of the biological characteristics of the 64 predicted targets of TFCOM, the FC, CC, and BP enrichment analyses of the assumed targets were performed to simplify the important biological processes ($p < 0.01$) as shown in Figures 4(e)–4(h). The potential pathways related to the anticancer effect of TFCOM were further identified by the KEGG pathway enrichment analysis in which analysis was performed for 64 genes. Finally, a total of 20 enriched pathways were identified that were involved in the anticancer effect of TFCOM and are presented in Figures 4(e)–4(h). The results showed that 42 biological processes (BP) mainly included the response to cell proliferation, regulation of apoptotic signaling pathways, and senescence. Cellular components (CC), included the extracellular space, cytoplasm, protein complex, nuclear cytoplasm, and transcription factor complex. At the same time, molecular function (MF) consists of protein binding, enzyme binding, growth factor activity, DNA binding transcriptional activation activity, etc., and the top 20 pathways in each category.

In order to further identify the target proteins acting on the disease, the corresponding pathway information was obtained based on KEEG and other databases, and the corresponding 20 pathways were predicted (Figure 4(h)). As shown in Figure 4, 20 overlapping gene symbols and signaling pathways involved in apoptosis, migration, invasion, and proliferation in tumor complications include the PI3K-Akt signaling pathway, FAK signaling pathway, FOXO signaling pathway, HIF-1 signaling pathway, TNF signaling pathway, and other pathways involved in regulating the disease. It suggests that these targets interact with each other among different signals and are involved in disease regulation and life-sustaining activities.

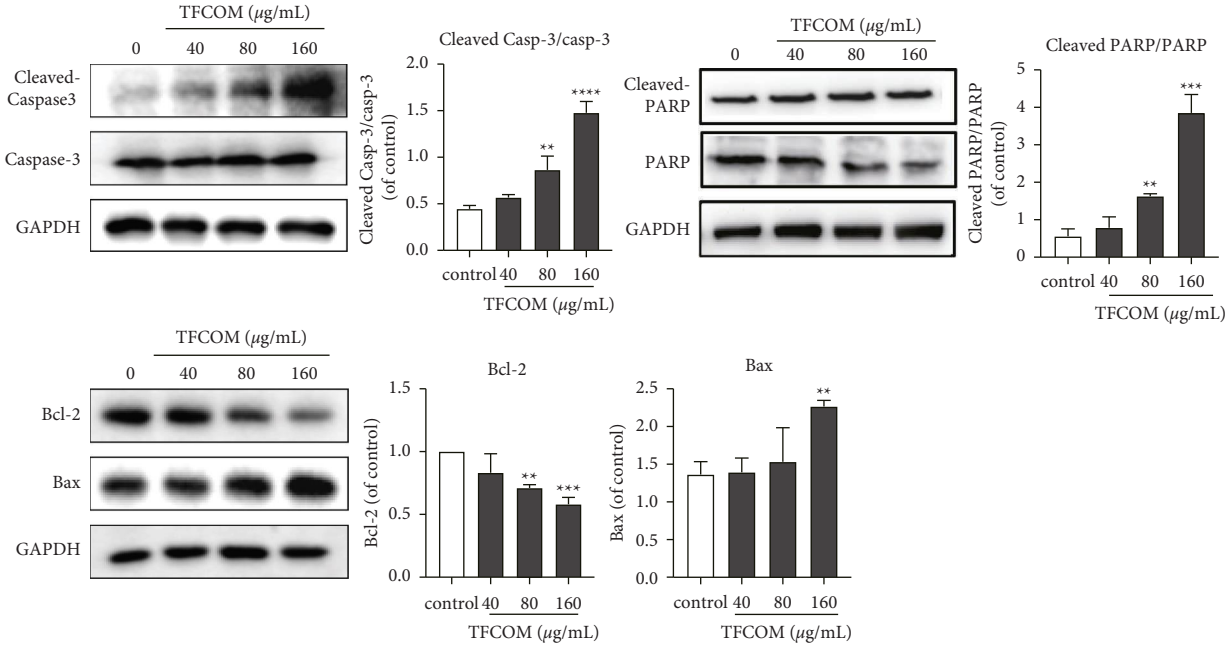
3.5. TFCOM Inhibited the FAK Phosphorylation and Downregulated the S1PR2 Expression. Next, we want to assess the



(a)



(b)



(c)

Figure 3: Continued.

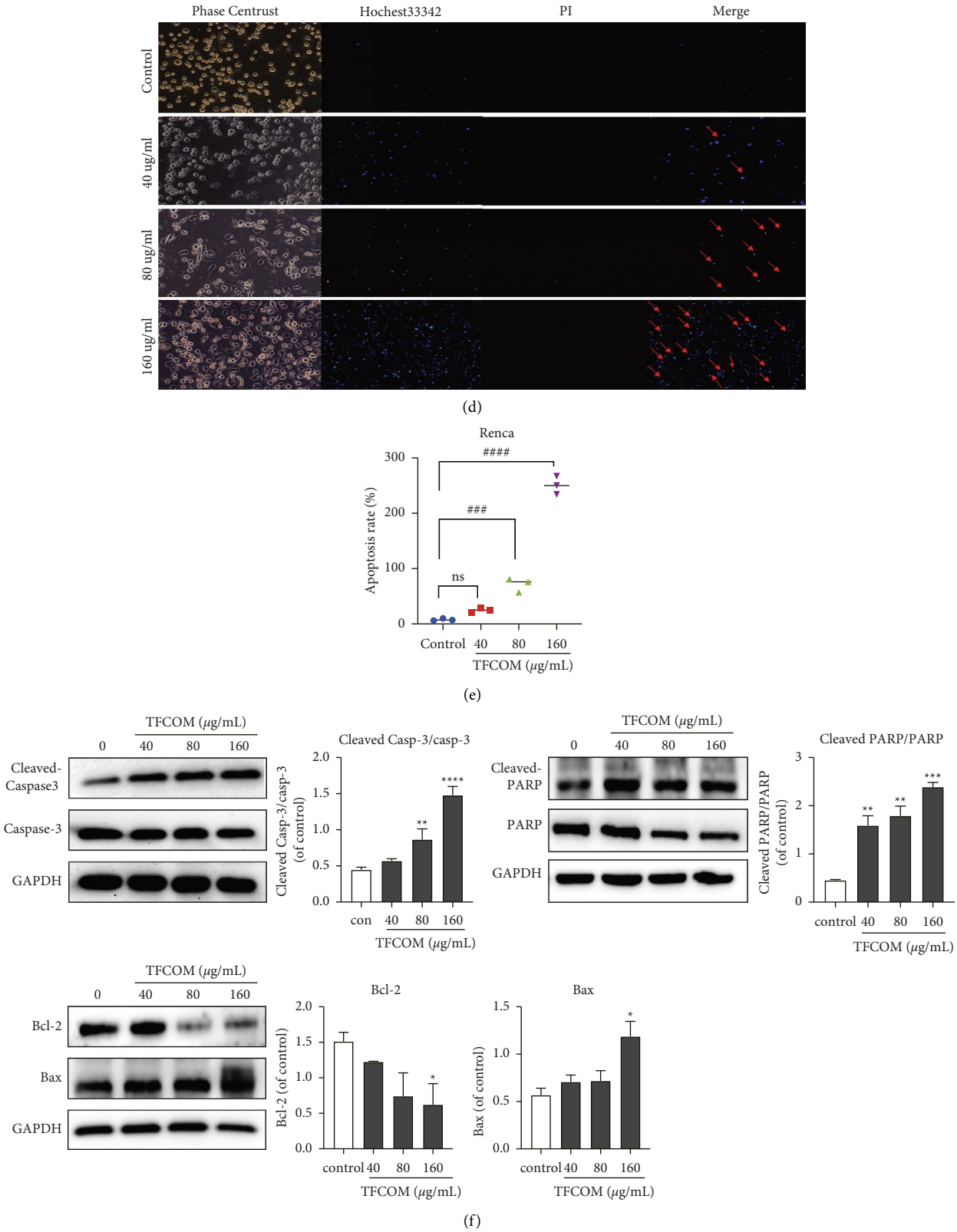


Figure 3: TFCOM induced apoptosis of 786-O and Renca cells. (a) The apoptotic cell of 786-o cells was examined by the Hoechst 33342 staining assay. (b) Rate of apoptosis cells. (c) Expression of protein associated apoptosis was checked in 786-O cells treated with TFCOM for 48 h by western blotting. Expression of BAX, cleaved-PARP, and cleaved-caspase 3 was upregulated while the ratio of PARP, caspase-3, and expression of Bcl-2 was reduced. Experiments were performed in triplicate. (d) The apoptotic cell of Renca was examined by Hoechst 33342 staining assay. (e) Rate of apoptosis cells. (f) Expression of protein-associated apoptosis was checked in Renca cells treated with TFCOM for 48 h by western blotting. Expression of BAX, p53, cleaved-PARP, and cleaved-caspase 3 was upregulated while the ratio of PARP, caspase-3, and expression of Bcl-2 was reduced. Experiments were performed in triplicate. Changes in the levels of BAX, Bcl-2, cleaved-PARP/PARP, and caspase-3/cleaved-caspase-3 proteins after being normalized to the levels of GAPDH were presented. Data are shown as mean ± SD of three independent experiments. $^{*}p < 0.05$, $^{**}p < 0.01$, $^{***}p < 0.001$ and $^{****}p < 0.0001$, as compared with the nontreated control.

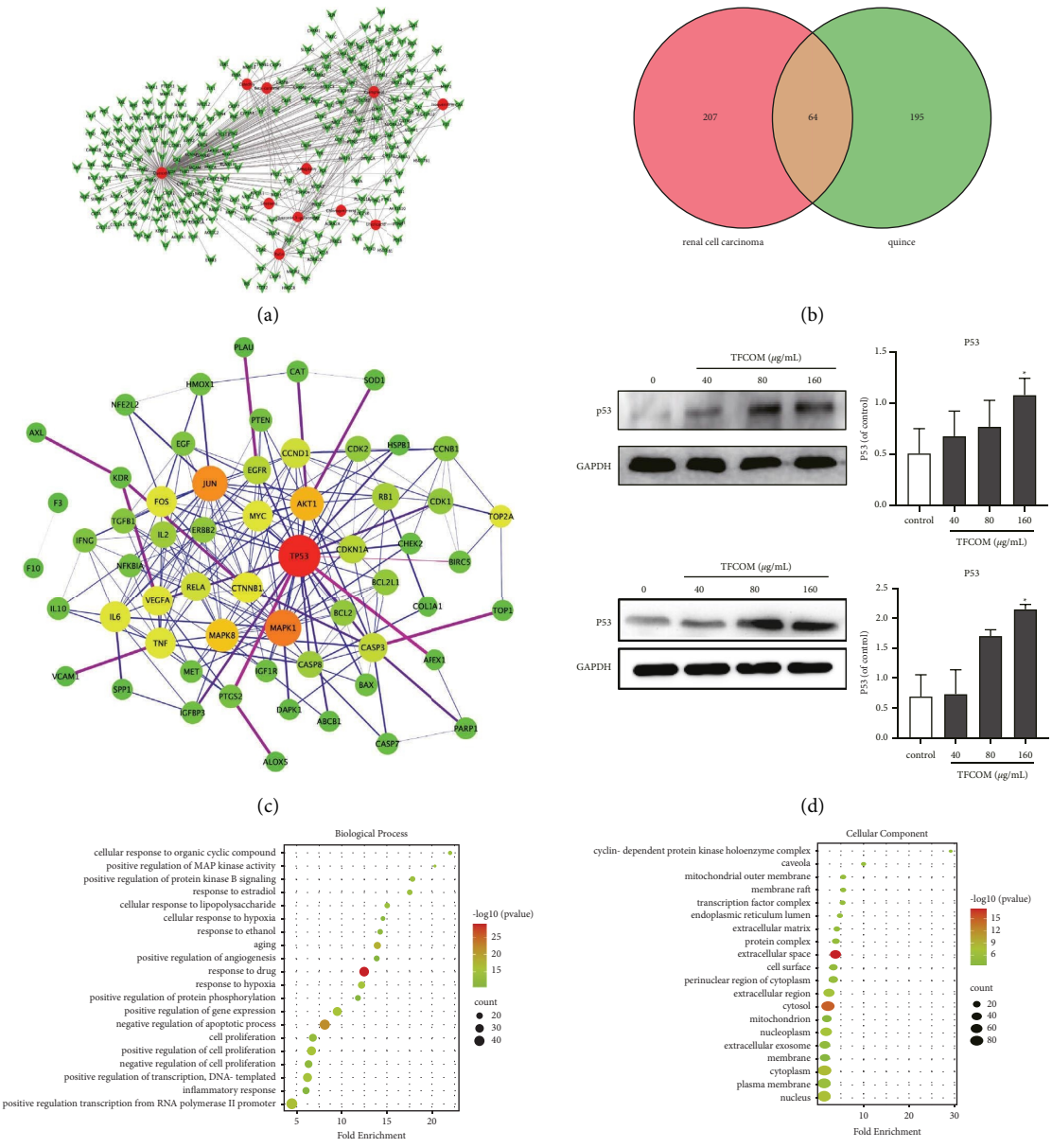
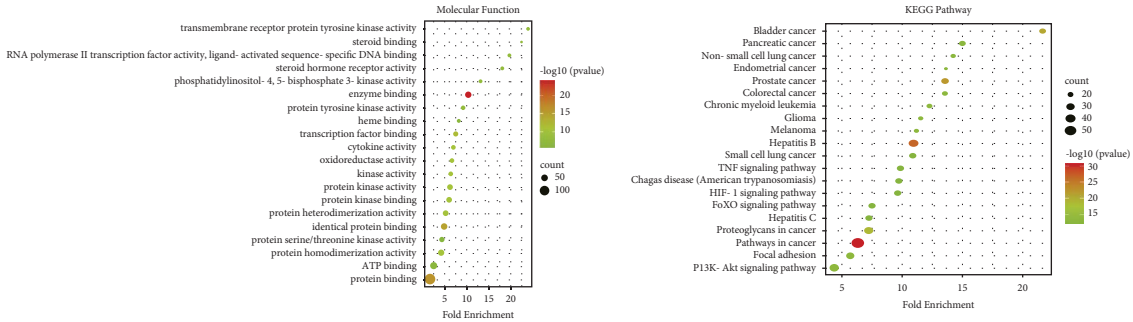


Figure 4: Continued.



(g) (h)

FIGURE 4: (a) Prediction and screening results of targets of active ingredients in renal cell carcinoma. The node size indicates the importance of the node in the network. (b) Analyses of the drug-ingredient-gene symbol-disease network. RCC and TFCOM share common target Venny diagram. (c) Protein-protein interaction network and the network of interactions between active components and corresponding targets. The color scale indicates the p value, and the dot size indicates the gene count in each term. (d) Changes in the levels of p53 proteins after being normalized to the levels of GAPDH. Data are shown as mean ± SD of three independent experiments. $^{*}p < 0.05$, $^{**}p < 0.01$ as compared with the nontreated control group. (e) GO analysis of the biological process (BP), mitotic G1 DNA damage checkpoint, G1 DNA damage checkpoint, and mitotic G1/S transition checkpoint were screened out. (f) GO analysis in the cellular component category; cyclin-dependent protein kinase holoenzyme complex, serine/threonine kinase complex, and protein kinase complex were obtained. (g) GO analysis in the molecular function category. (h) KEGG analysis, CXCR chemokine receptor binding, and sulfur compound binding were screened out.

effect of TFCOM on the pathway and cell migration. Furthermore, FAK expression was checked by western blotting, and the result showed that the expression of P-FAK was decreased in the cells treated with the TFCOM extract in dose-dependent manner (Figures 5(a) and 5(c)). In addition, according to previous studies, FAK phosphorylation in RCC cells is dependent on the S1P/S1PR2 axis. Therefore, we also studied the changes of TFCOM to S1PR2. The results showed that the expression level of S1PR2 was also significantly decreased, which suggested that FAK/S1PR2 was involved in the migration of 786-O and Renca cells inhibited by TFCOM. Taken together, TFCOM may be involved in the inhibition of the migration of RCC cells *via* regulating FAK/S1PR2 signaling pathways.

3.6. TFCOM Regulated the Expression of WNT/β-Catenin Signaling Pathway. In cancer, the upregulation of WNT/β-catenin pathway reported that it is involved in cell proliferation, apoptosis, and migration. As a result of WNT/β-catenin pathway activation the transactivation of genes through WNT target genes, c-Myc, and cyclin D1 induce [21]. In addition, our PPI network results show that C-Myc may be one of the potential mechanisms of TFCOM anticancer effects. Wnt3a/β-catenin/C-myc expression was checked by western blotting, and the result clarified that the expression of Wnt3a, β-catenin, and C-myc was decreased while GSK-3β was increased in the cells treated with TFCOM in dose-dependent manner (Figures 6(a) and 6(c)). As a result, TFCOM was most likely to affect the proliferation, apoptosis, and migration of tumor cells by regulating the Wnt3a/β-catenin and C-myc signaling pathways.

3.7. TFCOM Regulated the Expression of PI3K/AKT/mTOR Signaling Pathway. KEGG result showed that PI3K-AKT signaling pathway may mediate the anticancer effects of TFCOM and participate in the regulation of cancer cell proliferation and transformation. Furthermore, PI3K/AKT and mTOR expressions were checked by western blotting, and the results clarified that the expressions of p-PI3K, p-AKT, and p-mTOR were decreased in TFCOM-treated cells in a dose-dependent manner. Taken together, TFCOM may inhibit migration and proliferation of 786-O and Renca cells by regulating PI3K/AKT and mTOR signaling pathways. Conversely, the expression levels of total AKT and total mTOR were not altered (Figures 7(a) and 7(c)).

4. Discussion

RCC is one of the common malignant tumors, which is mainly characterized by poor prognosis and late diagnosis with frequent recurrences [22]. For RCC, the primary therapy is surgical removal followed by chemotherapy or radiotherapy. However, these therapeutic practices have no major effect on the life-quality improvement of patients suffering from RCC [23, 24].

Therefore, there is an important need for more investigations about the pathology and therapy regarding RCC. At present, different genes have been identified which play a major role during RCC tumorigenesis. However, the important genes differ between the reports which may be due to the heterogeneity of the disease [25]. In the current study, we found that TFCOM significantly inhibited proliferation and migration and induced apoptosis of RCC cells. TFCOM induces apoptosis by changing the expression level of apoptosis-related proteins and inhibiting RCC proliferation and migration through the FAK/S1PR2 and PI3K/AKT/mTOR pathways. In addition, the proliferation of RCC cells was inhibited by Wnt/β-catenin/c-myc signaling pathway. Thus, TFCOM can inhibit RCC cell migration and proliferation by inducing apoptosis and inhibited migration.

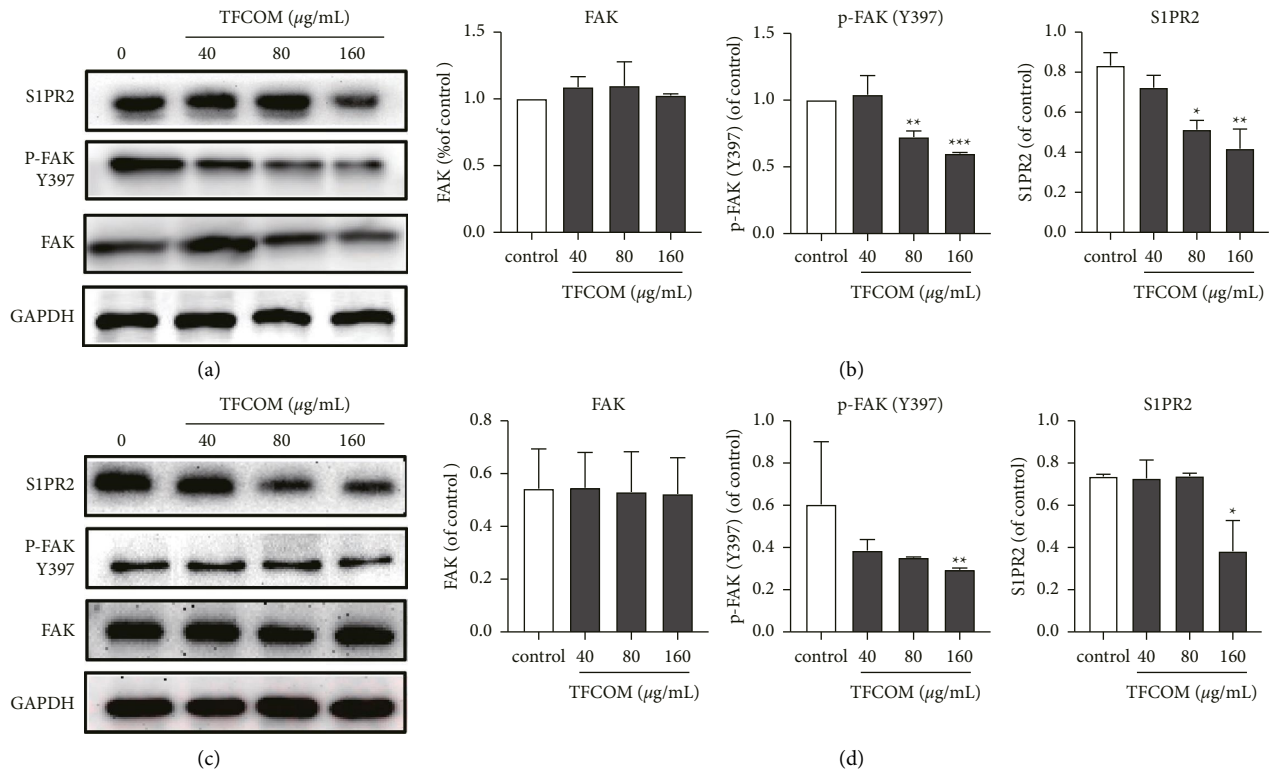


Figure 5: TFCOM inhibited migration of RCC by regulating S1PR2/FAK signaling pathway. (a) Protein level of migration is checked on 786-O cells treated with TFCOM extract 48 h. S1PR2/p-FAK is consistently reduced after being treated by TFCOM. (b) Changes in the levels of S1PR2/FAK proteins after being normalized to the levels of GAPDH are presented. (c) Protein level of migration is checked on Renca cells treated with TFCOM 48 h. S1PR2/p-FAK was consistently reduced after being treated with TFCOM. (d) Changes in the levels of S1PR2/FAK proteins after being normalized to the levels of GAPDH are presented. Data are shown as mean ± SD of three independent experiments. $^{*}p < 0.05$, **, $p < 0.01$ $^{***}p < 0.001$ as compared with the nontreated control group.

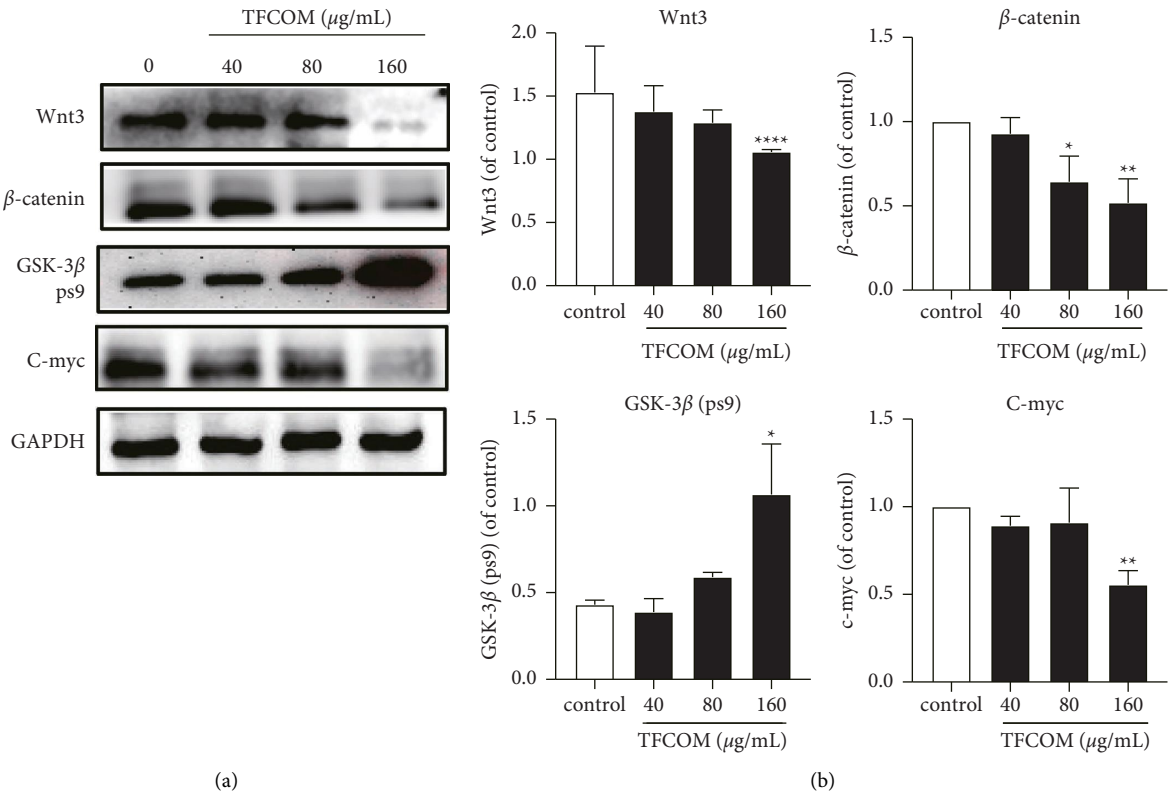


Figure 6: Continued.

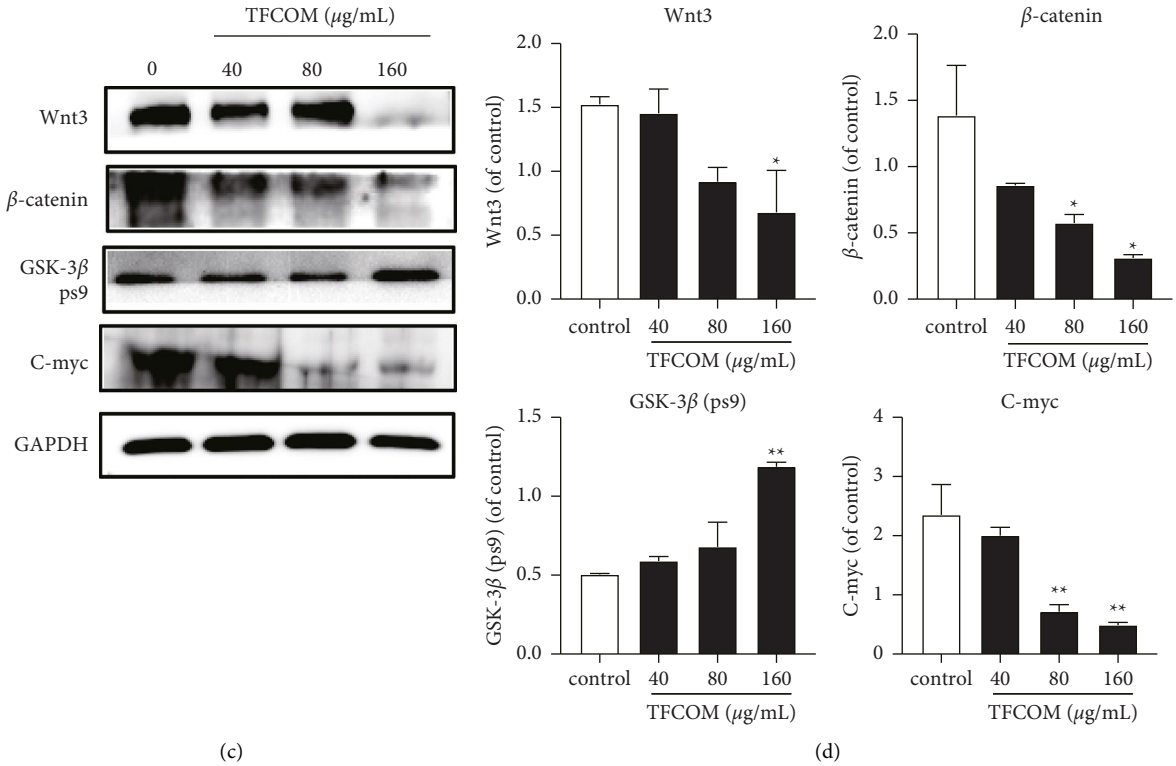


Figure 6: TFCOM inhibited proliferation and migration of RCC by regulating Wnt/β-catenin signaling pathway. (a, c) Protein level checked on 786-O and Renca cells that are treated with TFCOM for 48 h. Wnt/β-catenin/c-myc consistently reduced, and GSK-3β is increased after being treated with TFCOM. (b, d) Changes in the levels of proteins after being normalized to the levels of GAPDH are presented. $^{*}p < 0.05$, $^{**}p < 0.01$ $^{****}p < 0.0001$.

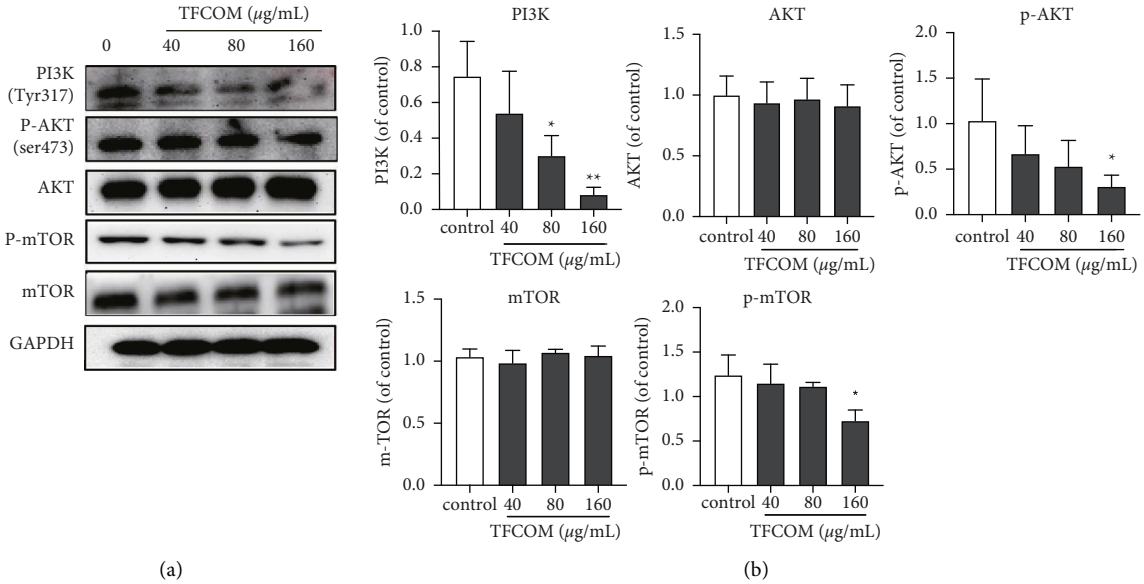


Figure 7: Continued.

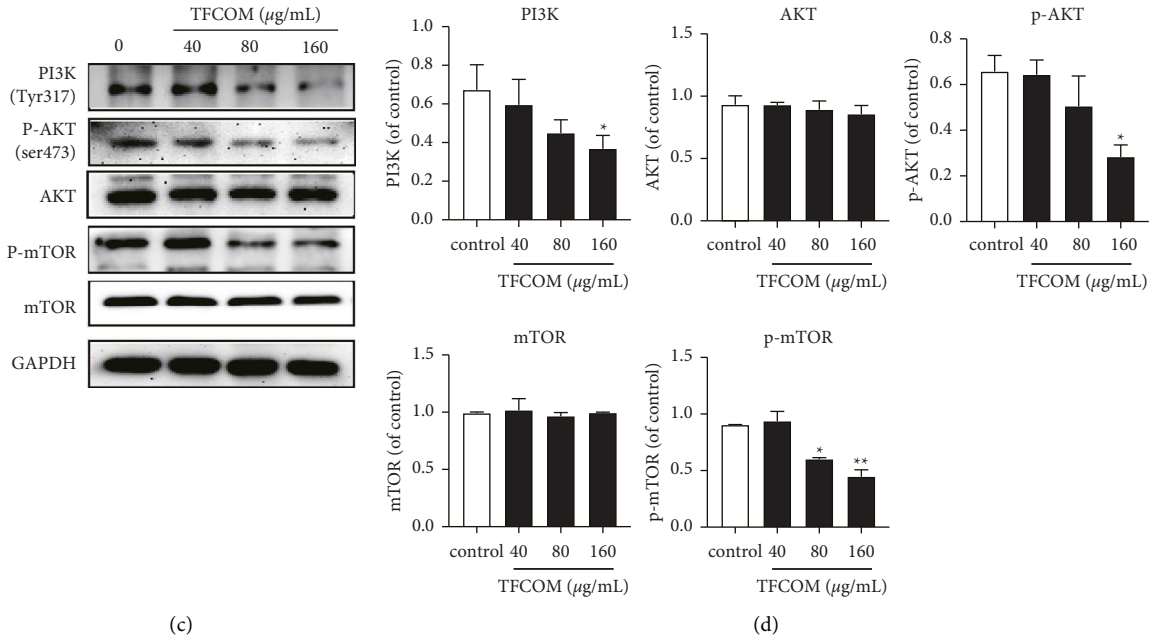


Figure 7: (a, c) Protein level is checked on 786-O and Renca cells that are treated with TFCOM for 48 h. PI3K/AKT/mTOR is consistently reduced after being treated with TFCOM. (b, d) Changes in the levels of proteins after being normalized to the levels of GAPDH, data are shown as mean ± SD of three independent experiments. $^{*}p < 0.05$, $^{**}p < 0.01$ as compared with the nontreated control.

Natural products usually have good antitumor activity and safety characteristics. In recent years, *C. oblonga* was reported to have potent antitumor activity. The antiproliferative activity of standardized ethanolic extract of *C. oblonga* leaf, fruit pellet, and flower petals was investigated against breast cancer cell line BT-20, hepatocellular carcinoma cell line HepG2 and colorectal adenocarcinoma cell line Caco-2. The study results indicated that *C. oblonga* leaf extract shows a powerful reaction against the viability of cancer cells. The *C. oblonga* fruit pellet extracts recorded up to 70% inhibitory effect on HepG2 cell viability, as well as 40% inhibitory rate against Caco-2 cells and 19% inhibitory rate against BT-20 cell proliferation. It is clear that *C. oblonga* has an excellent antiproliferative potency against cancer cells [15]. In the current study, we found that TFCOM inhibited RCC cell proliferation *in vitro* and revealed the underlying mechanisms. We calculated that the IC50 of TFCOM was 93.19 μg/mL for 786-O cells and 62.54 μg/mL for Renca cells. Therefore, TFCOM has better antiproliferation activity in RCC cells than that of the other tested cancer cell lines.

C. oblonga was reported to induce apoptosis and inhibit cell proliferation in cancer cells. The possible antitumoral effect of the *C. oblonga* polyphenolic extract of pulp and peel was investigated on human colon adenocarcinoma LS174 cells. MTT, LDH, flow cytometry, fluorescent probe, real-time quantitative PCR, and enzyme-linked immunosorbent assay were used for measuring different cell parameters. The antiproliferative activities of *C. oblonga* polyphenolic extract of the pulp and peel were observed with the highest efficiency [26]. The apoptosis induction was followed by inhibition of the NF-κB activity and by suppressing the angiogenic effector VEGF-A expression. The study concluded the action of the *C. oblonga* polyphenolic extract of pulp and peel exhibits a strong synergetic inhibitory action on cell viability in combination with 5-FU [27]. The effect of *C. oblonga* on colorectal cancer was also described by Benarba and Pandiella [28]. Here, in our study, we found that TFCOM significantly induced apoptosis in 786-O and Renca cell lines. TFCOM reduced the protein levels of PARP, caspase-3, and Bcl-2, and increase cleaved-caspase-3, cleaved-PARP, Bax, and p53 (Figure 8).

The role of GSK-3β and Wnt in tumors has been fully confirmed, which are involved in the regulation of tumor cell proliferation, invasion, and metastasis [29, 30]. GSK-3β acts as a switch in the Wnt signaling pathway, activating or deactivating the Wnt signaling pathway by phosphorylation of the substrate. GSK-3β is a key kinase determining the G-catenin phosphorylation, which promotes the phosphorylation of β-catenin by GSK-3β to be degraded by proteasome. Therefore, GSK-3β plays a tumor-suppressor role through β-catenin [31, 32]. Our results show that the expression of GSK-3β was increased while Wnt3a/β-catenin/C-myc was decreased after treatment with TFCOM. Collectively, these results suggest that TFCOM may regulate Wnt3a/β-catenin and GSK-3β signaling pathways and reduce the activity of 786-O and Renca, leading to inhibition of RCC cell proliferation.

FAK is expressed in most tissues and its sequence is highly conserved across species. The mouse (97% identity) and frog (90% identity) protein sequences are highly related in sequence to human FAK, while the zebrafish protein is conserved as well (79% identity). FAK is involved in the arrangement of integrins and building of FA via the catalysis of multiple downstream signals. This important enzyme is primitively dangerous when knocked out in mice and

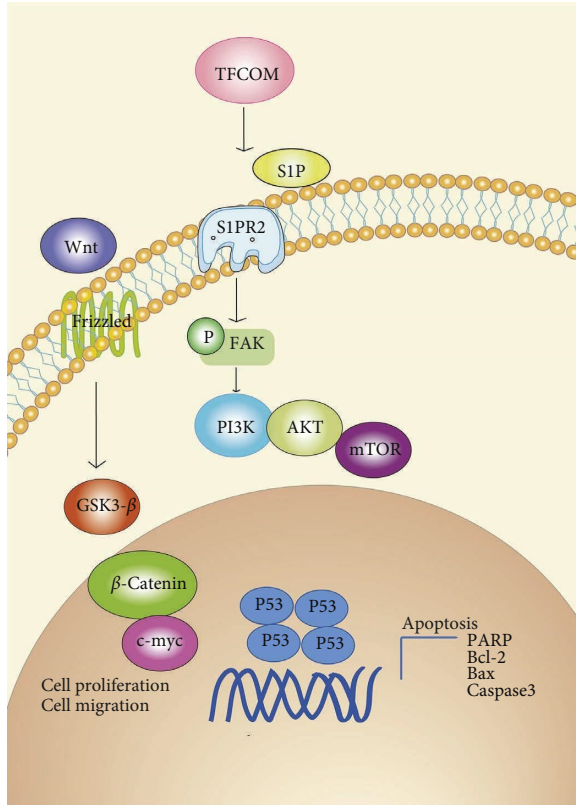


Figure 8: Schematic of proliferation, apoptosis, and migration induced by TFCOM via Wnt/β-catenin, S1PR2/FAK, and PI3K/AKT/mTOR signaling pathway. Our data suggest that TFCOM extract inhibits the migration of RCC by regulating S1PR2/FAK signaling pathway; TFCOM inhibits proliferation and migration by regulating PI3K/AKT/mTOR and Wnt/β-catenin signaling pathway; TFCOM induces apoptosis of RCC by regulating p53, Bax, Bcl-2, caspase 3, and PARP.

participates in the remodeling of the cytoskeleton and junctional complexes during multiple fundamental cell processes including migration, angiogenesis, and adhesion [33–35]. The enzyme which is responsible for the production of sphingosine 1-phosphate (S1P) is known as sphingosine kinase 1 (SK1). The overexpression of this enzyme is reported in different human solid tumors. Previously, it is reported that the enzyme may be involved in tumor cell proliferation, angiogenesis, survival, and invasion [36, 37]. However, its role is not reported clearly regarding clear-cell renal cell carcinoma (ccRCC). In 786-O ccRCC cells, the knockdown of SK1 resulted in no effect on the proliferation of cells. Alternatively, a decrease in the invasion and less phosphorylation of FAK have resulted from the knockdown. In addition, SK1 knockdown cells treated with S1P resulted in phosphorylation of FAK and invasion which was mediated by S1PR2 [38]. Similarly, some studies reported the role of SK1 by a cellular mechanism that involves S1P and S1PR2 which results in the phosphorylation of FAK. S1P has been shown to promote cell motility and FAK phosphorylation in human endothelial cells. The S1PR2/FAK axis has also been suggested to be involved in renal cancer cells' ability to invade [39, 40]. Particularly, the S1P/S1PR axis exhibits the main role in the activation of FAK/Src and p38 MAPK [41, 42]. On the other hand, it is reported that the activation of S1PR2 may also mediate the activation of S1P-augmented fibroblast chemotaxis via Rho-associated protein kinase (ROCK). However, the shRNA facilitates the silencing of SPHK1 resulting in colon cell apoptosis with the reduction in expression of FAK, p-FAK, intercellular adhesion molecule 1 (ICAM1), and vascular cell adhesion protein 1(VCAM1) specifying that SPHK1 is involved in the apoptosis resistance and progression of the CRC via FAK pathway, ICAM1, and VCAM1 [43]. Interestingly, our data also showed that the expression of P-FAK and S1PR2 decreased after the treatment with TFCOM, which suggested that TFCOM may inhibit 786-O and Renca cell migration by regulating S1PR2 to inhibit FAK phosphorylation. In addition, it has been reported that S1P activates S1PR1 and S1PR2, while S1PR1 activates JAK/STAT signal and S1PR2 activates FAK/PI3K/AKT signaling pathway. Our data also showed that PI3K/AKT and mTOR expression levels were also changed after TFCOM stimulation.

5. Conclusion

TFCOM has antitumor effects on RCC cells *in vitro*; it inhibits cell proliferation and promotes apoptosis. Moreover, we found that TFCOM inhibits S1PR2 expression and FAK phosphorylation, preventing the activation of the downstream Wnt3a/β-catenin/c-Myc and PI3K/AKT/mTOR pathways (Figure 8).

Data Availability

The data that support the findings of this study are available from the corresponding author upon reasonable request.

Conflicts of Interest

The authors declare that they have no conflicts of interest.

Authors' Contributions

MN completed the experiments and wrote the primary manuscript. NK assisted part of the experiment and editing. BZ and KA assisted part of the experiment. PY designed the research and revised the manuscript. WZ was involved in conceptualization, funding acquisition, project administration, and resource management.

Acknowledgments

The authors appreciate the financial support from the National Natural Science Foundation of China (81660696), Tianshan Talents-Youth Science and Technology Innovation Talents Training Program of Xinjiang Autonomous Region (2022TSYCCX0035), "Fourteenth Five-Year Plan" Key Discipline Construction Project of Xinjiang Autonomous Region (2021), and the Key Laboratory of Xinjiang Autonomous Region (XJDX1713). The authors would also like to thank Yilixiati Xiaokaiti for his cooperation in the English writing correction of the article.

References

[1] W. M. Linehan and C. J. Ricketts, "The Cancer Genome Atlas of renal cell carcinoma: findings and clinical implications," *Nature Reviews Urology*, vol. 16, no. 9, pp. 539–552, 2019.

[2] J. J. Hsieh, B. J. Manley, N. Khan, J. Gao, M. I. Carlo, and E. H. Cheng, "Overcome tumor heterogeneity-imposed therapeutic barriers through convergent genomic biomarker discovery: a braided cancer river model of kidney cancer. Paper presented at the Seminars in cell & developmental biology," *Seminars in Cell & Developmental Biology*, vol. 9, no. 64, pp. 5–7, 2017.

[3] I. Bozic, J. G. Reiter, B. Allen et al., "Evolutionary dynamics of cancer in response to targeted combination therapy," *Elife*, vol. 2, Article ID e00747, 2013.

[4] J. J. Hsieh, M. P. Purdue, S. Signoretti et al., "Renal cell carcinoma," *Nature Reviews Disease Primers*, vol. 3, no. 1, Article ID 17009, 2017.

[5] A. M. Molina, D. R. Feldman, M. H. Voss et al., "Phase 1 trial of everolimus plus sunitinib in patients with metastatic renal cell carcinoma," *Cancer*, vol. 118, no. 7, pp. 1868–1876, 2012.

[6] S. Mitra and R. Dash, "Natural products for the management and prevention of breast cancer. Evidence-Based Complementary and Alternative Medicine," *Evidence-based Complementary and Alternative Medicine*, vol. 26, 2018.

[7] J. Burns, T. Yokota, H. Ashihara, M. E. J. Lean, and A. Crozier, "Plant foods and herbal sources of resveratrol," *Journal of Agricultural and Food Chemistry*, vol. 50, no. 11, pp. 3337–3340, 2002.

[8] D. R. Mans, A. B. Rocha, and G. Schwartsmann, "Anti-cancer drug discovery and development in Brazil: targeted plant collection as a rational strategy to acquire candidate anti-cancer compounds," *The Oncologist*, vol. 5, pp. 185–198, 2000.

[9] S. Sabir, R. Qureshi, M. Arshad et al., "Pharmacognostic and clinical aspects of Cydonia oblonga: a review," *Asian Pacific Journal of Tropical Disease*, vol. 5, no. 11, pp. 850–855, 2015.

[10] U. Ashraf, G. Muhammad, M. Hussain, S. Bukhari, and M. Cydonia oblonga, "A medicinal plant rich in phytonutrients for pharmaceuticals," *Frontiers in Pharmacology*, vol. 7, no. 163, pp. 1–20, 2016.

[11] E. Sezik, E. Yesilada, G. Honda, Y. Takaishi, Y. Takeda, and T. Tanaka, "Traditional medicine in Turkey X. Folk medicine in central anatolia," *Journal of Ethnopharmacology*, vol. 75, no. 2-3, pp. 95–115, 2001.

[12] M. Ghafourian, P. Tamri, and A. Hemmati, "Enhancement of human skin fibroblasts proliferation as a result of treating with quince seed mucilage," *Jundishapur Journal of Natural Pharmaceutical Products*, vol. 10, no. 1, Article ID 18820, 2015.

[13] W. Zhou, A. Abdurahman, A. Umar et al., "Effects of Cydonia oblonga Miller extracts on blood hemostasis, coagulation and fibrinolysis in mice, and experimental thrombosis in rats," *Journal of Ethnopharmacology*, vol. 154, no. 1, pp. 163–169, 2014.

[14] F. Aliasl, T. Toliyat, A. Mohammadi et al., "Medicinal properties of Cydonia oblonga mill fruit (pulp and peel) in Iranian traditional medicine and modern phytothrapy," *Traditional and Integrative Medicine*, vol. 1, pp. 122–128, 2016, https://doaj.org/article/7ce028051d21495b9bb82489453723d0.

[15] L. Pirvu, A. Stefaniu, G. Neagu, B. Albu, and L. Pintilie, "In Vitro Cytotoxic and Antiproliferative Activity of Cydonia oblonga flower petals, leaf and fruit pellet ethanolic extracts. Docking simulation of the active flavonoids on anti-apoptotic protein Bcl-2," *Open Chemistry*, vol. 16, no. 1, pp. 591–604, 2018.

[16] W. Zhou, E. Abdusalam, P. Abliz et al., "Effect of Cydonia oblonga Mill. fruit and leaf extracts on blood pressure and blood rheology in renal hypertensive rats," *Journal of Ethnopharmacology*, vol. 152, no. 3, pp. 464–469, 2014.

[17] M. Minaiyan, M. Parvan, and S. E. Sajjadi, "Protective effect of two extracts of Cydonia oblonga Miller (quince) fruits on gastric ulcer induced by indomethacin in rats," *International Journal of Preventive Medicine*, vol. 8, no. 1, 2017.

[18] A. Umar, G. Iskandar, A. Aikemu et al., "Effects of Cydonia oblonga Miller leaf and fruit flavonoids on blood lipids and anti-oxydant potential in hyperlipidemia rats," *Journal of Ethnopharmacology*, vol. 169, pp. 239–243, 2015.

[19] M. Carvalho, B. M. Silva, R. Silva, P. Valentao, P. B. Andrade, and M. L. Bastos, "First report on Cydonia oblonga Miller anticancer potential: differential antiproliferative effect against human kidney and colon cancer cells," *Journal of Agricultural and Food Chemistry*, vol. 58, no. 6, pp. 3366–3370, 2010.

[20] Z. Li, Y. Tang, S. Zhu et al., "Ethanol extract of Patrinia scabiosaefolia induces the death of human renal cell carcinoma 786-O cells via SIRT-1 and mTOR signaling-mediated metabolic disruptions," *Oncology Reports*, vol. 39, no. 2, pp. 764–772, 2018.

[21] U. A. Jimilia, Y. Ma'erdan, M. Nuribia, N. Muhads, and W. Zhou, "Based on network pharmacology, the therapeutic effect and target of the main active ingredient of xinjiang quince on non-small cell lung cancer were predicted," *Chinese Journal of New Drugs*, vol. 29, no. 19, 2020.

[22] N. N. C. Institute, "Cancer facts & figures 2020," *CA: A Cancer Journal for Clinicians*, vol. 70, pp. 1–76, 2020.

[23] S. W. Berquist, K. Yim, S. T. Ryan et al., "Systemic therapy in the management of localized and locally advanced renal cell carcinoma: current state and future perspectives," *International Journal of Urology*, vol. 26, no. 5, pp. 532–542, 2019.

[24] P. Wiechno, J. Kucharz, M. Sadowska et al., "Contemporary treatment of metastatic renal cell carcinoma," *Medical Oncology*, vol. 35, no. 12, pp. 156–211, 2018.

[25] C. D'Avella, P. Abbosh, S. K. Pal, and D. M. Geynisman, "Mutations in renal cell carcinoma," *Urologic Oncology: Seminars and Original Investigations*, vol. 38, no. 10, pp. 763–773, 2020.

[26] I. Riahi-Chebbi, M. Haoues, M. Essafi et al., "Quince peel polyphenolic extract blocks human colon adenocarcinoma LS174 cell growth and potentiates 5-fluorouracil efficacy," *Cancer Cell International*, vol. 16, no. 1, pp. 1–15, 2015.

[27] B. Benarba and A. Pandiella, "Colorectal cancer and medicinal plants: principle findings from recent studies," *Biomedicine & Pharmacotherapy*, vol. 107, pp. 408–423, 2018.

[28] I. Riahi-Chebbi, S. Souid, H. Othman et al., "The Phenolic compound Kaempferol overcomes 5-fluorouracil resistance in human resistant LS174 colon cancer cells," *Scientific Reports*, vol. 9, no. 1, pp. 195–220, 2019.

[29] Q. He, H. Yan, D. Wo et al., "Wnt3a suppresses Wnt/β-catenin signaling and cancer cell proliferation following serum deprivation," *Experimental Cell Research*, vol. 341, no. 1, pp. 32–41, 2016.

[30] M. Kim, A. Datta, P. Brakeman, W. Yu, and K. E. Mostov, "Polarity proteins PAR6 and aPKC regulate cell death through GSK-3 in 3D epithelial morphogen-esis," *Journal of Cell Science*, vol. 120, no. 14, pp. 2309–2317, 2007.

[31] R. Mancinelli, G. Carpino, S. Petrungaro et al., "Multifaceted roles of GSK-3 in cancer and autophagy-related diseases," *Oxidative Medicine and Cellular Longevity*, vol. 2017, Article ID 4629495, 14 pages, 2017.

[32] D. Wu and W. Pan, "GSK3: a multifaceted kinase in Wnt signaling," *Trends in Biochemical Sciences*, vol. 35, no. 3, pp. 161–168, 2010.

[33] M. C. Frame, H. Patel, B. Serrels, D. Lietha, and M. J. Eck, "The FERM domain: organizing the structure and function of FAK," *Nature Reviews Molecular Cell Biology*, vol. 11, no. 11, pp. 802–814, 2010.

[34] A. W. Orr and J. E. Murphy-Ullrich, "Regulation of endothelial cell function BY FAK and PYK2," *Frontiers in Bioscience*, vol. 9, no. 1-3, pp. 1254–1266, 2004.

[35] M. D. Schaller, "Cellular functions of FAK kinases: insight into molecular mechanisms and novel functions," *Journal of Cell Science*, vol. 123, no. 7, pp. 1007–1013, 2010.

[36] Y. A. Hannun and L. M. Obeid, "Principles of bioactive lipid signalling: lessons from sphingolipids," *Nature Reviews Molecular Cell Biology*, vol. 9, no. 2, pp. 139–150, 2008.

[37] M. Nagahashi, S. Ramachandran, E. Y. Kim et al., "Sphingosine-1-phosphate produced by sphingosine kinase 1 promotes breast cancer progression by stimulating angiogenesis and lymphangiogenesis," *Cancer Research*, vol. 72, no. 3, pp. 726–735, 2012.

[38] M. F. Salama, B. Carroll, M. Adada, M. Pulkoski-Gross, Y. A. Hannun, and L. M. Obeid, "A novel role of sphingosine kinase-1 in the invasion and angiogenesis of VHL mutant clear cell renal cell carcinoma," *The FASEB Journal*, vol. 29, no. 7, pp. 2803–2813, 2015.

[39] O.-H. Lee, D.-J. Lee, Y.-M. Kim et al., "Sphingosine 1-phosphate stimulates tyrosine phosphorylation of focal adhesion kinase and chemotactic motility of endothelial cells via the Gi protein-linked phospholipase C pathway," *Biochemical and Biophysical Research Communications*, vol. 268, no. 1, pp. 47–53, 2000.

[40] J. Zhao, P. A. Singleton, M. E. Brown, S. M. Dudek, and J. G. Garcia, "Phosphotyrosine protein dynamics in cell membrane rafts of sphingosine-1-phosphate-stimulated human endothelium: role in barrier enhancement," *Cellular Signalling*, vol. 21, no. 12, pp. 1945–1960, 2009.

[41] J. P. Hobson, H. M. Rosenfeldt, L. S. Barak et al., "Role of the sphingosine-1-phosphate receptor EDG-1 in PDGF-induced cell motility," *Science*, vol. 291, no. 5509, pp. 1800–1803, 2001.

[42] P. Quint, M. Ruan, L. Pederson et al., "Sphingosine 1-phosphate (S1P) receptors 1 and 2 coordinately induce mesenchymal cell migration through S1P activation of complementary kinase pathways," *Journal of Biological Chemistry*, vol. 288, no. 8, pp. 5398–5406, 2013.

[43] R. S. A. Sattar, M. P. Sumi, A. Kumar et al., "S1P signaling, its interactions and cross-talks with other partners and therapeutic importance in colorectal cancer," *Cellular Signalling*, vol. 86, Article ID 110080, 2021.